9674 *Macromolecules* **2010**, *43*, 9674–9681
DOI: 10.1021/ma1017583

Macromolecules
ARTICLE

Ab Initio Kinetic Modeling of Living Anionic and Zwitterionic Chain Polymerization Mechanisms

Christoph Loschen* and Nikolaj Otte

Henkel AG & Co. KGaA, 40191 Düsseldorf, Germany

Eugene Radchenko

Department of Chemistry, M. V. Lomonosov Moscow State University, 119991 Moscow, Russia

Received August 4, 2010; Revised Manuscript Received October 19, 2010

ABSTRACT: A scale-bridging study of first-principles calculations and kinetic modeling has been carried out to investigate anionic and zwitterionic chain polymerizations. On the example of the industrially relevant ethyl α-cyanoacrylate, the initiation with anionic and neutral species focusing on the first stages of chain formation is studied. In the first part of our study, we use quantum chemical methods at the DFT level to study the initiation of polymerization with an anionic species (hydroxide anion), leading to anionic chain polymerization, and a neutral species (pyridine), leading to zwitterionic chain polymerization, respectively. The calculation of reaction barriers for the initiation step reveals that the addition of a hydroxide anion to a cyanoacrylate monomer is a barrier-less and strongly exothermic process whereas pyridine addition shows a significant barrier and is slightly endothermic. Subsequent calculations of the reaction energies and barriers of cyanoacrylate polymerization up to a degree of oligomerization of 5 ($X_n = 5$) show that both initiation reaction and subsequent addition of the next few monomers determine the reactivity and properties of cyanoacrylates. To quantify these findings we use in the second part of our study the results of the quantum chemical calculations to parametrize a kinetic study of the polymerization process of cyanoacrylates. Starting from monomers and initiators the polymerization of the cyanoacrylate and resulting molecular weight built up is simulated. The consequences of the differences in kinetic parameters of anionic and zwitterionic mechanisms on molecular weights and polymer properties are discussed.

Introduction

In combination with constantly increasing computer performance density functional theory (DFT) nowadays serves as an important tool for material science and polymer chemistry and allows for obtaining a lot of useful information, often complementary to experiments. However, DFT based approaches are limited regarding the system sizes and time scales under scrutiny. Therefore, combining computational simulations at different length and time scales with so-called scale-bridging approaches becomes increasingly important. We are presenting such an approach by combination of density functional theory and kinetic modeling in a mere *ab initio* approach, to elucidate the intricacies of the chain polymerization of cyanoacrylates, which are known to undergo a classical living anionic polymerization.[1]

Alkyl cyanoacrylate (CA) monomers have been used widely since the 1950ies in industrial applications due to their unique properties.[2] Mostly known as superglues they are sold as incredibly fast curing adhesives with enormous bond strengths on a variety of substrates. They found also use as wound closure adhesives as they stick excellently to human tissue thus offering an alternative to wound stitching. Tailor-made CA nanoparticles made by dispersion or emulsion polymerization have potential as drug carriers as they are biodegradable and their surface may be easily be functionalized.[3,4] An interesting niche application is in crime scene investigations where a monomer based spray may be used to visualize finger prints (so-called cyanoacrylate fuming).[5]

*Corresponding author. E-mail: christoph.loschen@henkel.com.

Although CAs are of significant industrial importance detailed knowledge of their initiation mechanism is still rare. Because of two strongly electron withdrawing groups CAs are highly reactive monomers that may be initiated by only trace amounts of bases and may polymerize by a virtually living anionic polymerization within seconds or less to high molecular weight chains of about $\sim 10^6$ g/mol.[6] The resulting propagating carbanionic species are extremely stable under ambient conditions which makes them useful for industrial adhesive applications. When using neutral nucleophiles as initiators as for example tertiary amines zwitterionic species are formed (Scheme 1).

CAs can also be polymerized and copolymerized radically in the presence of sufficient acidic inhibitors[7] though with lower rate constants ($k_p \approx 1600$ L mol^{-1} s^{-1} versus $k_p \approx 10^5$ L mol^{-1} s^{-1} [ref 8]), and some work remains to be done to clarify their reactivity toward radicals.[9]

An extensive set of experimental kinetic investigations on the ionic polymerization of CAs have been performed by Pepper et al.,[8,10−12] where the initiation process was investigated with respect to the influence of different tertiary amine initiators, pyridines and phosphines. They could show that chain initiation by neutral species is a process more complex than a simple interaction between initiator and one monomer molecule. It rather encompasses several distinctive propagation steps thereafter. In the case of pyridine, those steps are difficult to characterize experimentally and result in complex, composite rate constants and in a strong deviation of the final molecular weight from the theoretical one. Understanding these early steps of chain polymerization is however crucial: In the absence of termination

 Published on Web 11/11/2010

Scheme 1. Formation of Anionic and Zwitterionic Propagating Chains by Hydroxide and by Pyridine, Respectively

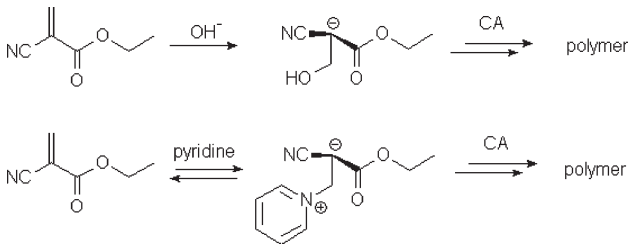

reactions and chain transfer reactions the evolution of the molecular weight distribution and thus the properties of the polymer are determined mainly by the initiation process. According to these studies CAs can undergo nearly living polymerizations[8] and thus elucidating their reactivity is of fundamental interest. Another severe difficulty during the experimental setup of CA polymerizations and especially for kinetic investigations is the purification of samples from synthesis byproducts and traces of stabilizers that may lead to irreproducible results.[8]

First-principle methods provide a natural means to study single chemical reactions such as the earliest steps of initiation and oligomerization: They provide accurate information on the structures of reactants and products and allow for the computation of reaction energies and if needed reaction barriers (when transition states are available). The reaction energetics thus calculated can be made into elementary kinetic rate constants using transition state theory, for example. Such a dedicated study of single reactions is not simple in experiment, since what is typically measured are apparent rates of reactions, which are a composite of rates of different elementary reaction steps. Thus, computationally derived, elementary rate constants, can be used to parametrize a model for chain polymerization kinetics, either based on deterministic integration of rate equations or based on stochastic Monte Carlo simulations.

Whether the set of model reactions is reasonable and meaningful for real-world systems can be tested by comparison of those properties which are also readily available experimentally, like molecular weights, their distribution or cross-link densities. Those properties again may serve as parameters for estimation of glass transition temperatures, mechanical moduli, and may even be a basis for finite elements simulations.

The combination of *ab initio* derived rate constants with kinetic modeling has recently been described as a paradigm shift[13] in polymer kinetic analysis because it allows the prediction of material properties by a truly first-principles based approach with methods which are nowadays readily at hand.

Several successful approaches have been reported in the past to predict kinetic rate constants for polymerization reactions based on quantum chemical calculations,[14] also pioneered by the work of Radom and co-workers.[15] As polymerization reactions are taking place either in bulk or in solution, solvent effects may strongly influence the rate constants. Recently, density functional studies of solvent effects on the tacticity of the free radical polymerization of methyl methacrylate[16] and on the rate constants of acrylamide polymerization in aqueous solution[17] have been published. In both cases, the effect of strong coordinating solvents had to be considered by incorporation of explicit solvent molecules into the calculation. For the case of less coordinating solvents the COSMO-RS approach delivered accurate results for the prediction of rate constants.[14]

However, quantum chemical computations on cyanoacrylates are rare and only a few have been published either concerning only radical polymerizations of acrylates and cyanoacrylates[18] or without considering chain lengths dependence of CA reactivity.[19] To the best of our knowledge, no rigorous quantum chemical study on the anionic polymerization of CAs exists so far.

The paper is organized as follows: First, we will shortly outline the underlying methods used in this study, then we will explain the model we constructed to elucidate the polymerization. Readers less interested in the technical details may proceed directly to the next section where we discuss the anionic versus zwitterionic chain propagation. The next section deals with the influence of the dielectric medium on the initiation reaction. We then discuss the reaction energetics of different basic initiators for CA initiation and finally the impact of the initiation on the overall polymerization kinetics.

Computational Details

Calculations of structures and reaction energies have been carried out at the HCTH level of theory[20,21] using numerical basis sets as implemented in the DMOL^3 code.[22,23] A basis set of double-ζ quality (DNP basis set) including polarization functions has been employed for geometry optimization if not stated otherwise. The optimization had been stopped after gradients have reached the convergence criterion of 0.002 au/Å. To account for the extended electron density of the occurring anionic species single point energies at the triple-ζ quality (TNP basis set) have been performed to obtain improved energies. The continuum solvent model COSMO[24,25] as available in DMOL^3 has been used to model the influence of the dielectric continuum assuming a dielectric constant of $\varepsilon = 7.6$ for the solvent THF.

To improve predictions for reaction barriers single point B3LYP[26] calculations with a TZVP basis,[27] respectivly on top of the HCTH/DNP structures have been performed with Turbomole.[28]

Transition states have been characterized by numerical calculation of second derivatives at the HCTH/DNP level by inspection of the normal modes with imaginary frequencies.

As the prediction of absolute rate constants better than to a factor of 10 is still almost impossible even with the most accurate quantum chemical methods,[29] we are working only with relative rate constants in this study. Though we may loose information about the absolute time frame of the reaction, we can be quite confident on the relative role of the contributing reaction channels. According to transition state theory the absolute rate constant of a reaction is given by the following relation:

$$k = \frac{k_B T}{h} e^{-\Delta G^{\ddagger}/RT} = \frac{k_B T}{h} e^{\Delta S^{\ddagger}/T} e^{-\Delta H^{\ddagger}/RT} \quad (1)$$

Here k_B is the Boltzmann constant, T is temperature, h is the Planck constant, R is the gas constant, $\Delta G^{\ddagger}$ the free energy, $\Delta S^{\ddagger}$ and $\Delta H^{\ddagger}$, the change in entropy and enthalpy at the transition state. For the relative rates of reaction 1 and 2 we thus obtain:

$$\frac{k_1}{k_2} = e^{(\Delta S_1^{\ddagger} - \Delta S_2^{\ddagger})/T} e^{-(\Delta H_1^{\ddagger} - \Delta H_2^{\ddagger})/RT} \quad (2)$$

As we are investigating reactions in a condensed medium, we may make the simplifying assumption that entropic effects dominated by the solvent environment contribute equally to both reactions, if the reactions are of a similar type, giving $\Delta S_1^{\ddagger} = \Delta S_2^{\ddagger}$. In cases where rotational, vibrational, and translational contributions to the enthalpy are of similar magnitude, the following working equation may be sufficient for our purposes:

$$\frac{k_1}{k_2} \approx e^{-(\Delta E_1^{\ddagger} - \Delta E_2^{\ddagger})/RT} \quad (3)$$

where $\Delta E^{\ddagger}$ is the electronic activation energy of the chemical reaction. The validity of this pragmatic approach is confirmed by the rather good agreement with experimental data. Estimates of relative rate constants have been obtained by quantum chemical

calculations of the reaction barriers and have been used for kinetic simulations as shown below to compute polymer properties.

Reaction energies ΔE have been obtained simply via energetic differences of all reactants and products.

Kinetic Modeling

The initiation and chain growth polymerization for this type of reaction are modeled by the following reaction equations, assuming that we have a classical living polymerization and neither chain transfer or termination reactions are important (Scheme 2):

Scheme 2. Reaction Equations for the Living Anionic Polymerization of Cyanoacrylates

$I + M \rightarrow P_1$	Initiation: k_1
$P_1 \rightarrow I + M$	Initiator Cleavage: k_2
$M + P_n \rightarrow P_{n+1}$	Monomer addition: k_3, k_5, k_7, (with n=1,2,3)
$P_{n+1} \rightarrow M + P_n$	Monomer cleavage: k_4, k_6, k_8 (with n=1,2,3)
$P_4 + M \rightarrow P, P + M \rightarrow P$	Polymerization: k_p (with n > 3)

Here I stands for initiator, M for monomer and P_n for the growing, living polymer chain with a degree of polymerization of $X_n = n$ and P for all chains with $n > 4$. In our case we have assumed that the rates for 5-mer formation and higher oligomers are already identical to the rate of polymerization. One then obtains the following set of coupled ordinary differential equations:

$$\frac{d[I]}{dt} = -k_1[M][I] + k_2[P_1] \quad (4)$$

$$\frac{d[M]}{dt} = -k_1[M][I] - k_3[M][P_1] - k_5[M][P_2] - k_7[M][P_3] - k_p[M][P_4] - k_p[M][P] + k_2[P_1] + k_4[P_2] + k_6[P_3] + k_8[P_4] \quad (5)$$

$$\frac{d[P_1]}{dt} = k_1[M][I] - k_2[P_1] - k_3[M][P_1] + k_4[P_2] \quad (6)$$

$$\frac{d[P_2]}{dt} = k_3[M][P_1] - k_4[P_2] - k_5[M][P_2] + k_6[P_3] \quad (7)$$

$$\frac{d[P_3]}{dt} = k_5[M][P_2] - k_6[P_3] - k_7[M][P_3] + k_8[P_4] \quad (8)$$

$$\frac{d[P_4]}{dt} = k_7[M][P_3] - k_8[P_4] - k_p[M][P_4] \quad (9)$$

$$\frac{d[P]}{dt} = k_p[M][P_4] + k_p[M][P] - k_p[M][P] = k_p[M][P_4] \quad (10)$$

Numerical integration yields the concentration of each of the species over time. The degree of polymerization and the number-average molecular weight is given by the amount of reacted species M built into the polymer chain. To obtain more detailed information about the molecular weight distribution it would have been necessary to keep track of each polymer chain with a certain chain length n, leading to a set of thousands of ordinary differential equations. Though it is nowadays possible to solve such equation systems[30] it was not considered necessary in our case. Another almost complementary approach to obtain weight distributions is via kinetic Monte Carlo simulations but can be very inefficient for reaction systems corresponding to stiff differential equations.

Quantum Chemical Model Construction and Benchmarking

As the anionic polymerization of CA is nearly a living polymerization with negligible termination or chain transfer reactions and a low polydispersity index it is an ideal model system. Another reason why ethyl α-cyanoacrylate is an ideal candidate for this kind of study is its practical relevance and, from a technical viewpoint, its few degrees of freedom which allow quite reliable assumptions to be made about the regio- and stereoselectivity of monomer addition. For the sake of simplicity we will deal only with low energy conformations, i.e., with complete *syndio* tacticity of the propagating chains and also consider only the *anti*-conformation of the CA backbone. The conformation of the added CA monomer is determined by a gas phase conformational search and being kept constant after addition. Note that only the conformation is kept, but no geometry constraints are being used for the calculations. By using these conformational constraints the main configuration of the growing chain can be determined in a unique way as shown in Figure 1 for both nucleophilic probes (OH^- and pyridine) used in the study.

We begin with studying the thermochemistry of the early steps of the chain polymerization reaction initiated by the hydroxide anion, and the successive addition of monomers to the propagating chain. By quantum-chemical calculation a sequence of reaction energies (ΔE_1, ΔE_2, ΔE_3, ..., ΔE_n) is obtained for each propagation step. For large n this value should correspond to the heat of polymerization.

In Figure 2, reaction energies at different level of theories are presented ranging from the highly exothermic initiation reaction with a hydroxide anion up to a degree of polymerization of $X_n = 5$. We see that at each theory level energies converge to a nearly constant value. This convergence is obtained for oligomeric chains with $X_n \approx 5$. The most drastic changes can be seen for the initiation reaction and the dimerization (ΔE, $X_1 \rightarrow X_2 \approx 50-70$ kcal/mol). We also note by comparison of the experimental enthalpies at 0K and 298 K, that finite temperature effects are in size of the error of the used density functionals, i.e. 5−10 kcal/mol.

To improve the model, we considered the screening of occurring charges by the dielectric surrounding. In our model system, we achieve this by using the conductor like screening model (COSMO)[24] with an dielectric constant of $\varepsilon = 7.6$ as obtained from the literature for THF, which might also be a suitable value for surrounding monomer during a bulk polymerization. Furthermore, the negative charge at the chain end might be incorrectly described by a basis set with just double-ζ quality. Therefore, also the effect of a better basis with triple-ζ quality (TNP) set was tested by performing single-point energy calculations on the as obtained structures (Figure 3). Going to a triple-ζ quality basis set leads to a significant decrease in the reaction energy, whereas the use of the COSMO approximation leads to an upward shift in reaction energies. The latter effect may be explained by screening of the electrostatic attractions of the two reacting species. The obtained reaction energies of all DFT functionals used are within the range of the experimentally determined values[31] for the heat of polymerization. Experimentally,[31] going from 0K ($\Delta H = 6.4$ kcal/mol) to room temperature ($\Delta H = 11.5$ kcal/mol) induces only a minor change of enthalpy with respect to the accuracy of common DFT functionals and shows that our chosen model suffices our practical purposes, especially as we are only interested in relative energy differences.

The computational determination of the enthalpy at 298.15 K for the final reaction step in this model, the formation of the 5mer,

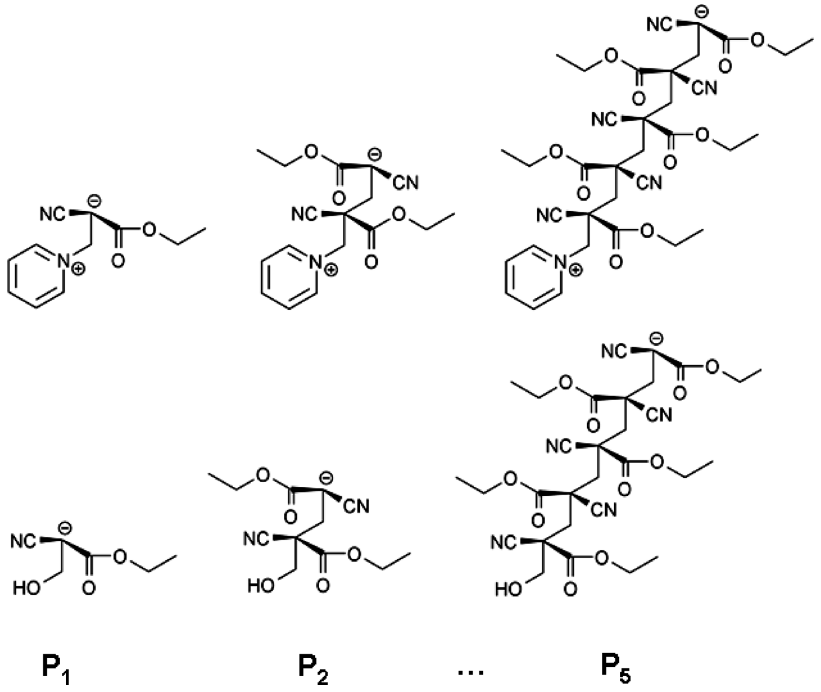

Figure 1. The model for the buildup of the cyanoacrylate propagating chain initiated by a hydroxide anion and by pyridine (with X_n = 1, 2, and 5). The conformations shown above are obtained via syndiotactic arrangement of the cyano- and ester-groups and *anti*-conformation of the polymer-backbone thus providing a structure with low conformational strain.

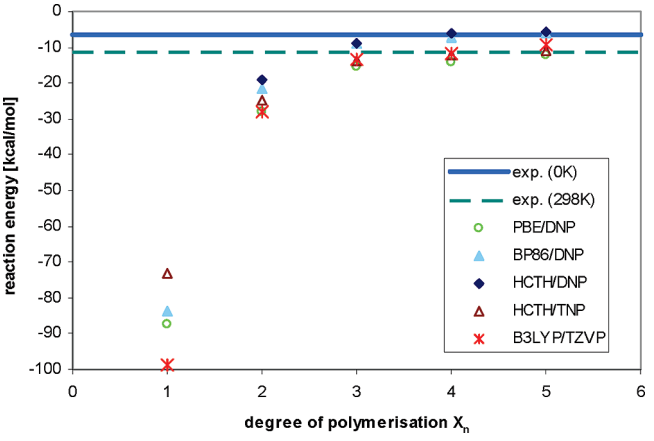

Figure 2. Calculated reaction energies [ΔE] for X_n of up to 5 for the anionic polymerization at different level of theories. Energies have been obtained as single point calculations on the HCTH/DNP optimized structures. Experimentally determined heat of polymerization is shown at 0 K (solid line) and at 298 K (dashed line) from ref 31.

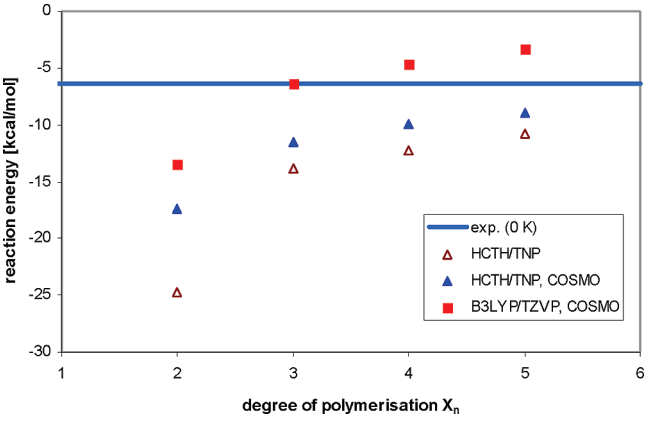

Figure 3. Calculated reaction energies [ΔE] for X_n up to 5 for the anionic polymerization by using larger basis sets of triple-ζ quality and by including the effect of a dielectric surrounding the growing chain (COSMO with $\varepsilon = 7.6$). The solid line shows the experimentally determined heat of polymerization at 0K (solid line).

gave $\Delta H(298.15\ \mathrm{K}) = -8.5$ kcal/mol, which is in fair agreement to the experimentally measured $\Delta H(298.15\ \mathrm{K}) = -11.5$ kcal/mol.[31] Because of the neglect of explicit condensed phase effects in our model the calculated entropy change for the reaction is far too strong ($\Delta S(298.15\ \mathrm{K}) = -51$ cal/mol) as compared to the experiment (($\Delta S(298.15\ \mathrm{K}) = -21$ cal/mol).[31] Consequently, calculated free energies would be estimated too positive within the model. As already argued above, those effects are negligible as long as we are only computing relative rate constants.[32]

Anionic versus Zwitterionic Polymerization

By addition of a neutral nucleophile to the cyanoacrylate monomer one obtains a zwitterionic species (Scheme 1). In another set of calculations we therefore compared the reaction energies by anionic and zwitterionic initiation up to $X_n = 5$ which is shown in Figure 4.

To generate a zwitterionic propagating species pyridine was selected as initiator. For pyridine, we now find an endothermic reaction for the first initiation step. Reaction energies however converge to a similar *negative* value as for the hydroxide case for higher degrees of polymerization. In a sense, the memory on how the reaction was initiated is lost with $\sim X_n = 5$. With other words, the chain starter may influence the chemistry at the chain end over up to four monomer units.

All zwitterionic species were obtained as stable structures from geometry optimizations. Furthermore, we did not find any hint for a prohibitive charge separation barrier during chain growth. Analysis of the quantum-chemically derived charges[33] for the zwitterion at the nitrogen and at the chain end carbon revealed that they are rather low ($\sim \pm 0.12$ e). Thus, it is justified to assume there is no such prohibitive charge separation barrier during chain growth.

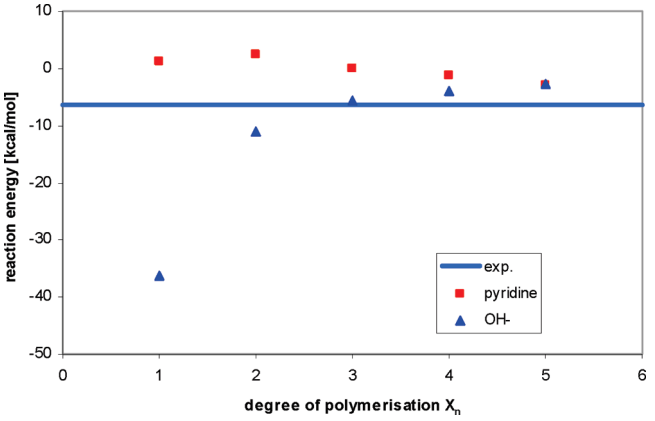

Figure 4. Calculated reaction energies [ΔE] for X_n of up to 5 for a chain initiated by pyridine and by a hydroxide anion, using B3LYP/TZVP and COSMO with $\varepsilon = 7.6$. The experimentally determined heat of polymerization at 0 K is shown as a solid line.

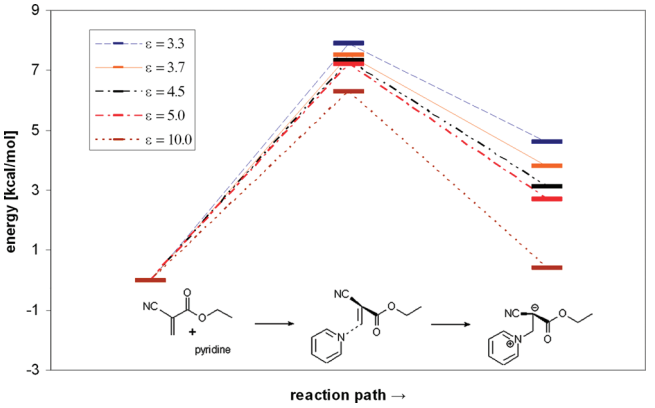

Figure 5. Calculated reaction barriers $\Delta E^{\ddagger}$ and reaction energies ΔE (B3LYP/TZVP) for pyridine initiation in dependence of the dielectric constant of the continuum solvent model (COSMO).

Influence of the Dielectric Continuum

An interesting finding was the necessity of using the solvent continuum model in order to obtain stable intermediates for the zwitterionic species. The zwitterionic species under scrutiny were *not* stable, i.e., were cleaved into reactants during geometry optimization under gas phase conditions. To shed more light on this issue, we have computed the impact of the change of the dielectric constant of the surrounding continuum on the reaction energies and reaction barriers of the pyridine initiation reaction.

Calculations as shown in Figure 5 reveal a clear trend: reaction energies as well as reaction barriers decrease when the dielectric constant increases.[34] This finding corresponds to the experimental fact that solvent polarity plays an important role for cyanoacrylate stability. For example going to more polar solvents with increasing dielectric constants may enhance CA initiation[39] or may slow down CA degradation.[35] Cronin et al. have reported that the rate constant for CA polymerization is decreased by a factor of 10 each by going from more polar THF ($\varepsilon = 7.6$) to diethyl ether ($\varepsilon = 4.3$) and finally to *n*-hexane ($\varepsilon = 1.89$).[39] We may also speculate that the overall decrease of the gross dielectric constant during polymer matrix build up may influence rates and chain lengths significantly. This may finally slow down or even stop polymerization.

Initiator Influence and Activation Barriers

To further elucidate the role of the initiator reactivity we performed quantum chemical calculations on the initiation reaction with different basic initiating compounds.

The B3LYP functional is well-known to give improved reaction barriers as compared with standard GGA functionals,[36] and can be used to give good relative ratios of reaction barriers, e.g., for the correct calculation of kinetic isotope effects.[37] In the following we are using this level to calculate some barriers for different nucleophilic probes: pyridine, OH^-, NMe_2^-, and $NHME_2$. This is done to take into account different reactivities of the initiator molecules. We use a weak neutral base (pyridine), a somewhat stronger neutral base ($NHME_2$) and strong anionic bases (OH^-, NMe_2^-). Please note that the amide and the amine nucleophiles are only chosen to assess their principal reactivity but are not of practical relevance. The first will not exist under ambient experimental conditions and the latter will undertake a reprotonation after addition to the monomer and thus quench the zwitterion, leading either to polymerization stop or to much more complicated kinetics.[38] In Table 1, the barriers and reaction energies of those bases with CA are presented. We have also included values for an enlarged basis set (TZVPP) to validate that our used basis TZVP is sufficiently converged.

For the two anions no reaction barriers could be found, they rather add barrier-less to the activated double bond. Please note that this is not an effect of an artificial high reactivity due to the neglect of solvent. In all calculations the well-established COSMO approximation has been used to account for solvent effects. Test calculations with an perfect screening by the solvent (i.e., using the dielectric constant of an conductor $\varepsilon =$ infinity) did also not lead to the successful location of a transition state.

Table 1 shows that we find the highest reaction barrier for the pyridine case, where as the somewhat better nucleophile $NHME_2$ gives a significant lower barrier. Taking also into account the shown HOMO energies, it becomes obvious that higher barriers for this reaction correspond to weaker nucleophiles, i.e., lower HOMO energies.

Relative rates for the reaction of pyridine with cyanoacrylate are shown in Table 2. Addition of pyridine and subsequent polymerization consists of several steps, the addition and dimerization being the rate determining one. The change of the reaction barrier with chain length is shown in Figure 6. It becomes obvious that the initiation and the dimerization have the highest barrier, subsequently the barrier decreases steadily. The activation energies for the pyridine initiated reaction were determined to be 4.8 kcal/mol for the addition of CA to the pyridine terminated 4-mer. These low barriers can be overcome easily at room temperature and are in good agreement with the observation that polymerization is slower than for the anionic polymerization but still take place within seconds.

We could not find any barriers for the strongly exothermic reactions of the anionic probe molecules like OH^- with CA (and e.g. similarly CH_3^-). Consequently those processes resulting in a free anionic propagating chain seem to be diffusion controlled during the initiation stage. Similarly no barriers could be found for CA addition to the anionic oligomers with chain lengths of 1, 2, and 3. For the addition of the CA monomer to the anionic 4mer moiety it was however possible to locate a reaction barrier of 2.5 kcal/mol.

According to the simulation results a neutral water molecule gives no stable product with cyanoacrylate, this finding corresponds to the experimental fact that cyanoacrylate polymerization in solution are stable up to 200 ppm water content.[39]

Computation of the addition of a tertiary amine model like NMe_3 to CA yields an endothermic reaction (+13 kcal/mol). No transition state could be located for the addition and thus no detectable barrier for the reverse reaction, i.e. the fragmentation. Thus, no direct product is likely to be found; instead, the amine would act as an initiator in the presence of humidity indirectly by the formation of hydroxide anions.

Table 1. Reaction Energies and Reaction Barriers for Different Nucleophiles Attacking the Cyanoacrylate at the Initiation Step[a]

	B3LYP/TZVP		B3LYP/TZVPP		
nucleophile	$\Delta E^{\#}$ [kcal/mol]	ΔE [kcal/mol]	$\Delta E^{\#}$ [kcal/mol]	ΔE [kcal/mol]	HOMO [eV]
pyridine	6.0	1.2	6.5	1.4	−7.28
OH^-	0.0	−36.2	0.0	−36.4	−3.88
$NHMe_2$	1.7	−6.8	2.5	−5.7	−6.14
NMe_2^-	0.0	−45.3	0.0	−44.6	−3.51

[a] HOMO (highest occupied molecular orbital) energies are also given (B3LYP/TZVP). For all calculations the COSMO approximation was used with $\varepsilon = 7.6$.

Table 2. Relative Reaction Rate Constants from Quantum-Chemically Computed Reaction Energies and Barriers (B3LYP/TZVP+COSMO) for the Pyridine Initiation k_1, the Oligomerization Reactions k_3, k_5, and k_7, the Corresponding Reverse Reactions k_2, k_4, k_6, and k_8, and for the Polymerization k_p (See also Scheme 2)[a]

reaction	$I + M \rightarrow P_1$	$P_1 \rightarrow I + M$	$M + P_1 \rightarrow P_2$	$P_2 \rightarrow M + P_1$	$M + P_2 \rightarrow P_3$	$P_3 \rightarrow M + P_2$	$M + P_3 \rightarrow P_4$	$P_4 \rightarrow M + P_3$	$P_n + M \rightarrow P_n$
barrier [kcal/mol]	6.0	4.8	7.6	5.3	6.8	6.9	5.9	7.2	4.8
rate constants k, relative	k_1 0.03	k_2 0.26	k_3 0.002	k_4 0.11	k_5 0.01	k_6 0.01	k_7 0.04	k_8 0.005	k_p 1.0

[a] For OH^- no barriers for the initial reaction steps have been found, and those are probably diffusion controlled, leaving the polymerization barrier with 2.5 kcal/mol as the rate determining step.

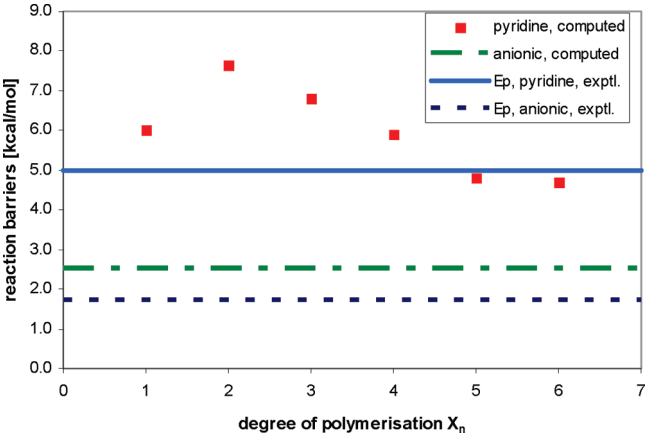

Figure 6. Calculated reaction barriers $\Delta E^{\ddagger}$ (B3LYP/TZVP+COSMO) for pyridine initiation in dependence of the chain length of the oligomers and the calculated reaction barrier for the anionic polymerization (irregular dashed line). The experimental values for activation energies of polymerization E_P as determined from ref 39 (pyridine initiation, solid line) and ref 6 (free anion case, dashed line) are given in comparison.

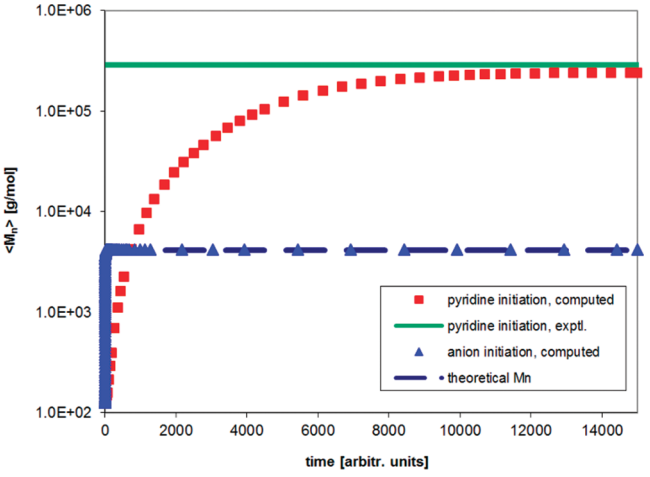

Figure 7. Molecular weight build up obtained from the rate equation integration, with relative rates as shown in Table 2. Pyridine initiation and anionic (OH^-) initiation are compared. The initiator:monomer ratio was kept constant at 1:33, leading to a theoretical $\langle M_n \rangle$ of 4125 g/mol.

We may conclude that initiation of CA via strong nucleophilic species is a rapid diffusion controlled process, with the chain propagation being the rate-determining step with a rather low barrier. Weak nucleophiles or neutral bases like pyridine, however, show a complete different and more complicated picture: with the initiation and the dimerization being rate determining and a somewhat slower polymerization process as compared to the free anion case.

Kinetic Simulations

In order to investigate the interplay between the initiator reactivity, its concentration, and the polymer build-up, we have assumed a simple kinetic scheme for this model system based on our findings from the quantum chemical calculations (Scheme 2).

In our model, we consider the following types of reactions with individual relative rate constants: the initiation reaction, the corresponding cleavage of the initiator, the oligomerization steps up to $X_n = 4$ with the corresponding cleavage of monomer and finally the polymerization. The monomer activation and the oligomerization steps are reversible in this model. The relative rates for those reactions can be found in Table 2 for the pyridine initiated reaction and the free anion case, modeled with OH^- as initiator. It was assumed that for large degrees of polymerization the rate of the zwitterionic polymerization approaches the one of the anionic polymerization. We note that according to the DFT calculations the dimerization is rate determining (k_2), though the monomer activation shows also a high barrier, i.e., low rate constant (k_1).

On the basis of those rates and on the rate equations of Scheme 2, we have modeled the polymer weight built up, as shown in Figure 7.

For a large difference between the rate-determining step and the rate of polymerization (k_2/k_p), as in the zwitterionic case, we see a significantly increased buildup of average molecular weight, because effectively less initiator molecules are available. Furthermore, we see also a larger time lag before the buildup of molecular weight takes place as compared to the anionically initiated systems. On a logarithmic scale we roughly reproduce the difference between the theoretical ([CA]/[initiator] = $DP_{theor.}$ = 33) and experimental degree of polymerization (DP = 2300) reported in ref 40.

In Figure 8, concentrations of some polymerization intermediates are shown, relative to the monomer concentration which has been chosen to be 1.0. Referring to a logarithmic ordinate we see

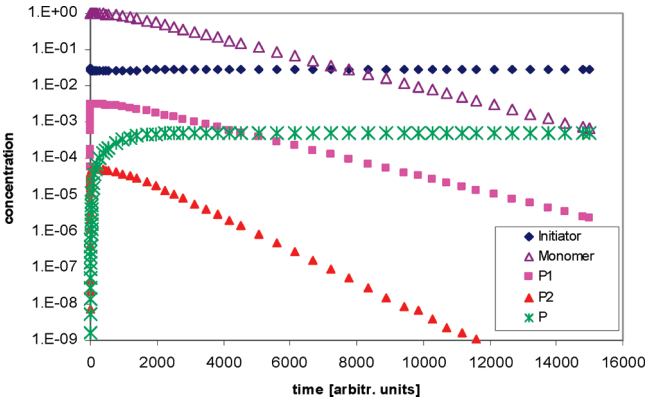

Figure 8. Different intermediate concentrations as resulting from the rate equation integration, with relative rates as shown in Table 1.

that the initiator concentration does not change much during the reaction. As the initiator amount remains constant so does the concentration of the propagating chains P. Intermediates P_1 and P_2 are formed at the beginning and during the course of the reaction and their concentration readily decreases, as they are consumed by the fast polymerization. Concentrations P_3 and P_4 are already so low that have not been shown and may easily approximated by a steady state approach. Decisive for the polymerization reaction is just the ratio of the rate-determining barrier, in this case the initiation and the dimer formation to the polymerization barrier.

Thus, based on the deviation of the theoretical degree of polymerization from the experimental one we may estimate the relative difference of the rate determining and the polymerization reaction barriers. For example for a ratio of [CA]/[initiator] = $X_{n,\mathrm{theor.}} = 33$ and an experimental $X_n \approx 2000$ as in ref 40, we obtain with our model a ratio of $k_2/k_p = 750$. This corresponds, using Arrhenius law, to a *difference* in activation energies of about $\Delta E_2^{\ddagger} - \Delta E_p^{\ddagger} = 4$ kcal/mol. This is only a rough approximation in which the influence of pre-exponential Arrhenius factors is not included but is within the size regime of the computed values in Table 2.

Conclusions

We have constructed a first-principles based model system for ionic chain polymerization. With this model the thermochemistry of the cyanoacrylate polymerization can be accurately described and the computed results are in close agreement with experiment. The investigation of the chain propagation reveals that at a degree of polymerization X_n of about 4 to 5 reaction energies are nearly converged, which is valid for the anionic as well as for the zwitterionic propagating species. Thus, an intermediate regime prior to plain chain polymerization exists which connects the classical steps of initiation and polymerization. This kind of long-range effect via several monomer units might have interesting implications also for copolymerization studies.

For pyridine initiation leading to zwitterionic species, we find a reaction barrier of about 8 kcal/mol for the rate-determining step. This is significantly higher than for the free anion case which is diffusion controlled during initiation and has a barrier of about 2.5 kcal/mol for chain propagation. By combination of the quantum chemical data with kinetic modeling, we are able to unscramble the composite processes of initiation and early oligomerization. Accordingly, the strong deviation from the theoretical value of the average molecular weight as found for example in ref 40 may be explained by a slow, rate-determining initiation process followed by a rapid polymerization. This is in accordance with early experimental findings, labeled as the slow initiation no termination (SINT) process,[8] and also to recent results relating the initiator reactivity to the morphology of grown poly(ethyl cyanoacrylate) nanofibres.[41]

Another decisive control parameter identified is the solvent polarity or more generally, the dielectric surrounding the intermediate zwitterions. A polar environment should increase the stability of those moieties by a stronger dielectric screening of the Coulomb interactions of the two opposite charges. Thus, overall stability of the zwitterions is increased, the reaction barrier for initiation is lowered and chain propagation facilitated.

We have demonstrated that scale-bridging studies as presented above provide a useful means to obtain valuable insights into chain polymerization studies which are complementary to experiments. The approach may also be transferred to other polymerizing systems containing composite reactions during the initiation and early oligomerization.

Acknowledgment. [The authors would like to thank Dr. Ciarán McArdle and Dr. Philipp Spuhler for helpful discussion and Henkel AG & Co. KGaA, for the permission to publish this paper.]

Supporting Information Available: Text, scheme and table with additional energetics for de- and reprotonation reactions of zwitterions and tables of calculated molecular structures as *xyz*-matrices. This material is available free of charge via the Internet at http://pubs.acs.org.

References and Notes

(1) Szwarc, M. *J. Polym. Sci., Part A: Polym. Chem.* **1998**, *36*, 9.
(2) Coover, H. W.; Dreifus, D. W.; O'Connor, J. T. In *Handbook of Adhesives*, 3rd ed.; Skeist, I., Ed.; Van Nostrand Reinhold: New York, 1990; p 463.
(3) Díaz-Torres, R.; Castano, V.; Ganem-Quintanar, A.; Quintanar-Guerrero, D.; Rodríguez-Romo, S. *Nanotechnology* **2005**, *16*, 2612.
(4) Weiss, C. K.; Ziener, U.; Landfester, K. *Macromolecules* **2007**, *40*, 928.
(5) Wargacki, S. P.; Lewis, L. A.; Dadmun, M. D. *J. Forensic Sci.* **2007**, *52*, 1057.
(6) Pepper, D. C. *J. Polym. Sci. Pol. Sym.* **1978**, *62*, 65.
(7) Yamada, B.; Yoshioka, M.; Otsu, T. *Makromol. Chem.* **1983**, *184*, 1025.
(8) Pepper, D. C. *Polym. J.* **1980**, *12*, 629.
(9) There is some evidence that the cyano group may cause penultimate effects in radical co-polymerizations which may be the reason for inherently inconsistent literature values for the Alfrey-Price Q,e scheme for cyanoacrylates; see, e.g.: Cywart, D. A.; Tirrell, D. A. *J. Am. Chem. Soc.* **1989**, *111*, 7544.
(10) Johnston, D. S.; Pepper, D. C. *Makromol. Chem.* **1981**, *182*, 407–420.
(11) Pepper, D. C.; Ryan, B. *Makromol. Chem.* **1983**, *184*, 383.
(12) Pepper, D. C.; Ryan, B. *Makromol. Chem.* **1983**, *184*, 395.
(13) Coote, M. L.; Barner-Kowollik, C. *Aust. J. Chem.* **2006**, *59*, 712.
(14) Deglmann, P.; Müller, I.; Becker, F.; Schäfer, A.; Hungenberg, K.-H.; Weiss, H. *Macromol. React. Eng.* **2009**, *3*, 496.
(15) Heuts, J. P. A.; Gilbert, R. G.; Radom, L. *Macromolecules* **1995**, *28*, 8771.
(16) Degirmenci, I.; Eren, S.; Aviyente, V.; De Sterck, B.; Hemelsoet, K.; Van Speybroeck, V.; Waroquier, M. *Macromolecules* **2010**, *43*, 5602.
(17) De Sterck, B.; Vaneerdeweg, R.; Du Prez, F.; Waroquier, M.; Van Speybroeck, V. *Macromolecules* **2010**, *43*, 827.
(18) Degirmenci, I.; Aviyente, V.; Van Speybroeck, V.; Waroquier, M. *Macromolecules* **2009**, *42*, 3033.
(19) Zhou, Y.; Bei, F.; Ji, H.; Yang, X.; Lu, L.; Wang, X. *J. Mol. Struct.* **2005**, *737*, 117.
(20) Hamprecht, F. A.; Cohen, A. J.; Tozer, D. J.; Handy, N. C. *J. Chem. Phys.* **1998**, *109*, 6264.
(21) Boese, A. D.; Handy, N. C. *J. Chem. Phys.* **2001**, *114*, 5497.
(22) Delley, B. *J. Chem. Phys.* **1990**, *92*, 508.
(23) Delley, B. *J. Chem. Phys.* **2000**, *113*, 7756.
(24) Klamt, A. In *Encyclopedia of Computational Chemistry*, Schleyer, P. v. R., Allinger, L., Eds.; Wiley: New York, 1998, 604.
(25) Delley, B. *Mol. Simul.* **2006**, *32*, 117.

(26) Becke, A. D. *Phys. Rev. A* **1988**, *38*, 3098. (b) Lee, C.; Yang, W.; Parr, R. G. *Phys. Rev. B* **1988**, *37*, 785. (c) Becke, A. D. *J. Chem. Phys.* **1993**, *98*, 5648.
(27) Schäfer, A.; Huber, C.; Ahlrichs, R. *J. Chem. Phys.* **1994**, *100*, 5829.
(28) Ahlrichs, R.; Bär, M.; Häser, M.; Horn, H.; Kölmel, C. *Chem. Phys. Lett.* **1989**, *162*, 165.
(29) Jensen, F. *Introduction to Computational Chemistry*: John Wiley & Sons Ltd.: Chichester, U.K., 1999.
(30) Wulkow, M. *Macromol. React. Eng.* **2008**, *2*, 461.
(31) Bykova, T. A.; Kiparisova, Y. G.; Lebedev, B. V.; Mager, K. A.; Gololobov, Y. G. *Polymer Science* **1991**, *33*, 537.
(32) To improve overall accuracy, more sophisticated theoretical models like ab initio molecular dynamics would be necessary, however, causing in our opinion unwarranted additional effort and cost.
(33) Hirshfeld, F. L. *Theor. Chim. Acta* **1977**, *44*, 129.
(34) For dielectric constants $\varepsilon \leq 3.3$, severe SCF convergence problems occurred for the zwitterions.
(35) Han, M. G.; Kim, S.; Liu, S. X. *Polym. Degrad. Stab.* **2008**, *93*, 1243.
(36) Koch, W.; Holthausen, M. A. *Chemist's Guide to Density Functional Theory*: Wiley-VCH: Weinheim, Germany, 2001.
(37) Spuhler, P.; Holthausen, M. *Angew. Chem., Int. Ed.* **2003**, *42*, 5961.
(38) Klemarczyk, P. *Polymer* **2001**, *42*, 2837.
(39) Cronin, J. P.; Pepper, D. C. *Makromol. Chem.* **1988**, *189*, 85.
(40) Klemarczyk, P. *Polymer* **1998**, *39*, 173.
(41) Mankidy, P. J.; Rajagopalan, R.; Foley, H. C. *Polymer* **2008**, *49*, 2235.